Characterization of plasma-sprayed hydroxyapatite by ^{31}P-MAS-NMR and the effect of subsequent annealing

J. VOGEL, C. RÜSSEL, G. GÜNTHER
Friedrich-Schiller-Universität Jena, Otto-Schott-Institut, Fraunhoferstraße 6, D-07743 Jena, Germany

P. HARTMANN
Friedrich-Schiller-Universität Jena, Institut für Optik und Quantenelektronik, Max-Wien-Platz 1, D-07743 Jena, Germany

F. VIZETHUM, N. BERGNER
Friatec AG, Keramik- und Kunststoffwerke, Sparte Medizintechnik, Steinzeugstr. 50, Postfach 71 02 61, D-68229 Mannheim, Germany

The characterization of plasma spray induced changes become complicated by the formation of amorphous phases. ^{31}P magic angle spinning (MAS)-nuclear magnetic resonance (NMR) measurements are suited to detect both crystalline and amorphous calcium phosphates. Therefore, we used ^{31}P-MAS-NMR and X-ray diffraction (XRD) to characterize plasma-sprayed hydroxyapatite. Besides small quantities of nearly unchanged crystalline apatite, disordered partly X-ray amorphous apatite was detected. Additionally, a non-stoichiometric amorphous calcium phosphate phase possessing a structure similar to TCP, probably calcium enriched, was observed. No indications of tetracalciumphosphate could be found. The decomposition of apatite during plasma spraying is reversible. An additional annealing procedure of plasma-sprayed hydroxyapatite at suitable temperatures above 500 °C rebuilds crystalline apatite structure.

1. Introduction

Because of its advantageous *in vivo* behaviour, hydroxyapatite (HA) is one of the most successful implant materials [1, 2]. Lack of sufficient strength can be compensated by using it as a coating on metallic substrates. In the past few years, various coating techniques have been applied to produce HA layers [3], however, plasma spraying is favoured today. Plasma-sprayed HA coatings possess relatively high densities, and thicknesses of more than 50 μm can be achieved. The drawback of this method is the extremely high temperature of the plasma, leading to partial thermal decomposition of HA.

At nearly 900 °C, HA decomposes, evaporating water and forming partially or completely dehydroxylated oxy-(hydroxy)-apatite [4, 5]. Above 1050 °C, an equilibrium with tricalcium-phosphate (TCP, $Ca_3(PO_4)_2$) and tetracalciumphosphate (TeCP, $Ca_4(PO_4)_2O$) exists [6, 7]:

$$Ca_{10}(PO_4)_6OH \rightleftarrows 2Ca_3(PO_4)_2 + Ca_4(PO_4)_2O + H_2O$$

TCP melts at 1730 °C and TeCP melts incongruently at 1630 °C cleaving CaO. The characterization of changes induced by plasma spraying is complicated due to the formation of amorphous phases. Since these phases cannot be detected using X-ray diffraction the only phase observed is HA. It was thus often interpreted that the crystal structure of the initial HA is retained in the plasma sprayed layer. However, ^{31}P magic angle spinning (MAS)-nuclear magnetic resonance (NMR) measurements are suitable to detect both crystalline and amorphous calcium phosphates [8]. In this study we combined ^{31}P MAS-NMR and X-ray diffraction in order to analyse quantitatively the phase composition of plasma-sprayed HA as a function of additional annealing.

2. Experimental procedures

The initial hydroxyapatite powder (particle size 40–100 μm) was highly crystalline and stoichiometric. It was sprayed onto flat metallic substrates, the resulting coating having a thickness around 500 μm. The quantity of plasma-sprayed HA obtained was sufficient for annealing tests at various temperatures using an electrically heated furnace. Both initial HA and plasma-sprayed material were provided by FRIATEC AG, Germany.

α-TCP, β-TCP and TeCP were synthesized as references for the NMR investigations: β-TCP was

0957–4530

obtained by dropwise addition of the stoichiometric quantity of orthophosphoric acid to an aqueous suspension of calcium hydroxide. α-TCP was formed by annealing β-TCP at 1400 °C for 30 min and subsequent strong quenching of the product. TeCP was synthesized by annealing a stoichiometric mixture of $CaCO_3$ and β-TCP at 1620 °C for 15 min. X-ray powder patterns were collected using a Siemens diffractometer D 5000 (40 kV, 30 mA, scanning rate 0.02 degree/s, CuK_α radiation). For the exposure of the NMR spectra a Bruker AMX 400 NMR spectrometer was used. The MAS rotation rates amount to $\nu = 14$ kHz. A single pulse sequence ($\pi/2$ pulse lengths of $t_w = 1.5$ μs, delay times $t_{de} = 10$ μs, recycle times $t_{re} = 200$ s) was used and the chemical shifts are referenced to a solution of phosphoric acid (85%).

3. Results and discussion

3.1. Reference materials and initial HA

All reference materials and the initial hydroxyapatite were characterized by X-ray diffraction. Their spectra showed only the reflexes of the pure substances (α-TCP: JCPDS 9-348, β-TCP: JCPDS 9-169, TeCP: JCPDS 25-1137, HA: JCPDS 9-432).

Fig. 1 shows the ^{31}P NMR-MAS spectra of HA, α-TCP, β-TCP and TeCP. The ^{31}P NMR spectrum of hydroxyapatite possesses only a single line at $\delta_{iso} = 2.3$ ppm. In contrast, the spectra of the other calcium monophosphates investigated show three or more spectral components with significantly different line positions (Table I). The ^{31}P shift anisotropies obtained are typical of unprotonated monophosphates ($|\Delta\delta| < 50$ ppm) [9]. While the distinctions of HA, TCP and TeCP are well defined, the quantitative distinctions of α-TCP and β-TCP are difficult because of their overlapping lines.

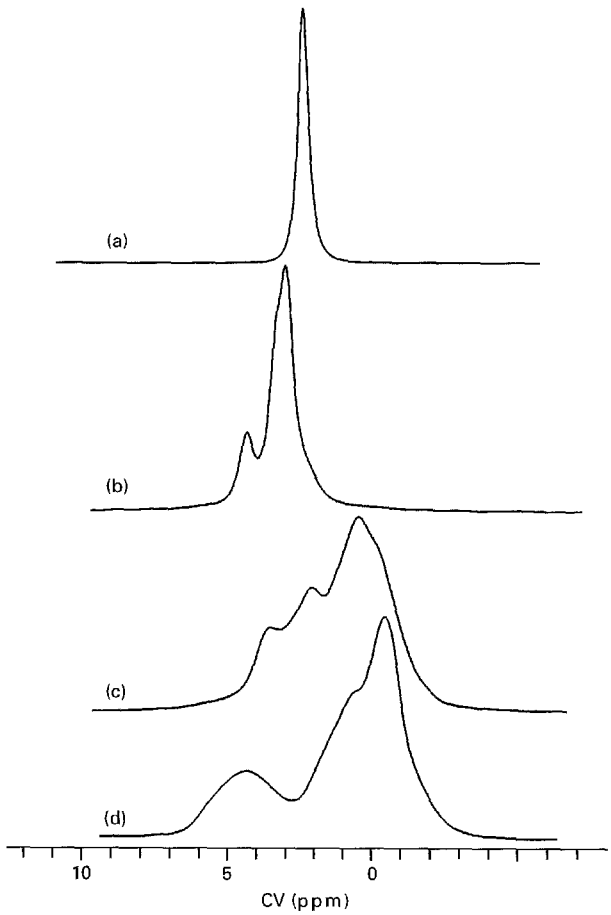

Figure 1 ^{31}P MAS-NMR spectra of different calcium monophosphates (resonant frequency $\nu_0 = 161.92$ MHz; spinning speed $\nu_r = 10.0$ kHz; receiver delay time $t_{de} = 10$ μs; pulse width $t_w = 1.5$ μs and repetition time $t_{re} = 300$ s) : (a) HA; (b) TECP; (c) α-TCP; (d) β-TCP.

3.2. Plasma-sprayed hydroxyapatite

Fig. 2 shows the X-ray diffraction pattern of hydroxyapatite before and after plasma spraying. The powder patterns seem to be similar and all lines observed can be attributed to the crystal phase hydroxy(oxy)apatite. However, the intensity of the HA-reflexes in the pattern of the plasma sprayed powder is reduced and the background is increased – an indication of amorphous phases. The enhanced line width, in principle, can be caused by both lattice distortion of the crystalline HA and a crystal size in the nanometre range.

The ^{31}P MAS-NMR spectra of the initial Fig. 1 and plasma-sprayed HA (Fig. 3) differ significantly. In contrast to the single-line NMR spectrum of crystalline apatite, the ^{31}P spectrum of plasma-sprayed HA possesses four lines (Table II). The values of the iso-

TABLE I ^{31}P chemical shift tensor parameters and relative intensities of several lines in different calcium monophosphates obtained by line fit analysis

Sample	δ_{iso} (ppm)	$\Delta\delta$ (ppm)	Line width (ppm)	Relative intensity (%)
Hydroxyapatite (HA)	2.3 ± 0.1	29 ± 5	0.4	100
Tetracalciumphosphate	4.3 ± 0.1		0.3	8 ± 1
(TECP)	3.1 ± 0.1		0.5	42 ± 4
	3.2 ± 0.1		1.5	50 ± 5
α-tricalciumphosphate	3.3 ± 0.2		1.0	12 ± 1
(α-TCP)	2.2 ± 0.2		0.7	9 ± 1
	0.5 ± 0.2		1.8	58 ± 6
	1.8 ± 0.4		5.2	20 ± 2
β-tricalciumphosphate	4.3 ± 0.2	40.0 ± 5	1.9	22 ± 2
(β-TCP)	0.3 ± 0.2	31.0 ± 5	2.5	67 ± 7
	−0.5 ± 0.2	35.5 ± 10	0.7	11 ± 1

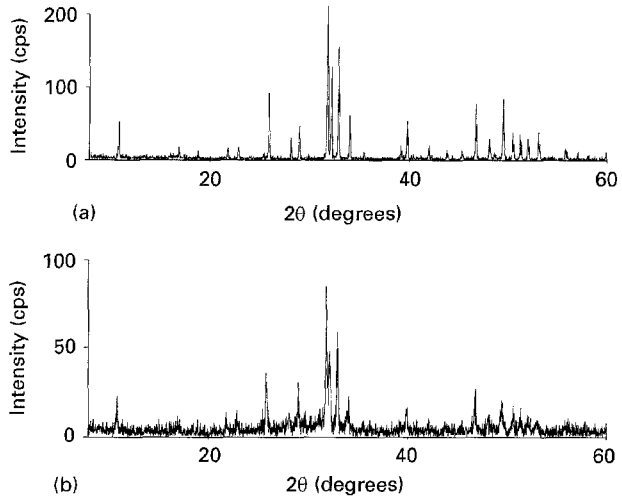

Figure 2 X-ray diffraction patterns of HA (a) before and (b) after plasma spraying (40 kV, 30 mA, scanning rate 0.02 degrees/s, CuK_α radiation).

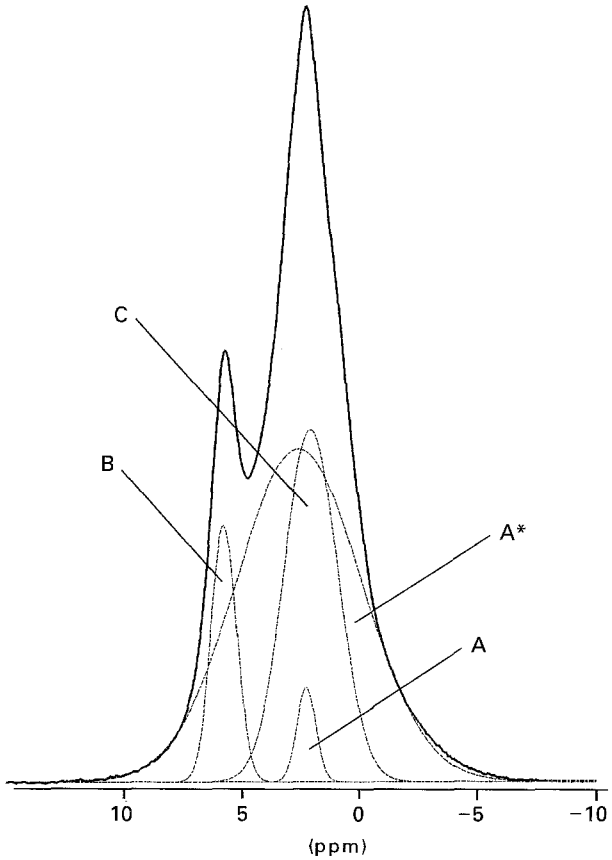

Figure 3 Experimental and simulated ^{31}P MAS-NMR spectra of crystalline HA and plasma-sprayed HA (resonant frequency $\nu_0 = 161.92$ MHz; spinning speed $\nu_r = 14.0$ kHz; receiver delay time $t_{de} = 10$ μs; pulse width $t_w = 1.5$ μs and repetition time $t_{re} = 200$ s).

tropic chemical shift for the two lines A and A* are typical of apatite. While the MAS line width of line A (0.4 ppm) is within the range usually observed for crystalline phases [8], the line width of A* (2.9 ppm) indicates considerable distortion of the HA structure. Around 4% of all phosphorous nuclei occur in crystalline and around 43% in disordered apatite.

Due to their significantly different isotropic chemical shifts the lines B and C belong to one or more additional phases. The values of the anisotropic chemical shift of these two lines ($|\Delta\delta| < 50$ ppm) are typical of unprotonated monophosphate structures influenced by calcium [9]. ^{31}P MAS-NMR spectra of annealed β-TCP (1800 °C for 10 min) showed isotropic shifts ($\delta_{iso}\{A\} = 5.1$ ppm, $\delta_{iso}\{B\} = 1.0$ ppm) slightly different from those of β-TCP. Therefore, both lines B and C are attributable to disordered tricalcium phosphate. However, no indications of tetracalciumphosphate can be found. Also, X-ray reflexes attributed to CaO cannot be detected. Hence, it is supposed, that the amorphous TCP phase is non-stoichiometric, possessing an excess of calcium. The absence of TeCP in the plasma-sprayed material is in contrast to results of other investigations [7, 10]. Probably, different plasma spray parameters influence the phase composition of the plasma-sprayed products.

Generally, hydroxyapatite is regarded as a bioactive non-resorbable implant material. However, the chemical stability and resistance to biological attack are clearly lowered by the plasma spray process [11]. This effect is caused by changed phase composition and lowered crystallinity of the plasma spray products. Therefore, displacement of the thermal decomposition equilibrium to the apatite side and an increase of crystallinity should be possible by annealing plasma-sprayed HA.

3.3. Annealed plasma-sprayed hydroxyapatite

The X-ray diffraction patterns of the plasma-sprayed HA and the annealed plasma-sprayed HA (900 °C for 3 h) are given in Fig. 4. The intensities of the apatite reflexes after annealing are notably higher, the background is decreased and the reflexes are relatively sharp. This means that the thermic decomposition of HA during plasma spraying is reversible. The ^{31}P NMR-MAS investigations confirm this conclusion. As seen in Fig. 5, the ^{31}P NMR spectrum

TABLE II Shift parameters and relative intensities of several lines in the ^{31}P NMR spectrum of the plasma-sprayed hydroxyapatite obtained by line fit analysis

Line	δ_{iso} (ppm)	Line width (ppm)	Relative intensity (%)	Structure
A	2.1 ± 0.1	0.4	4.3 ± 0.5	Crystalline HA
A*	2.4 ± 0.3	2.9	43.3 ± 5	Distorted HA
B	5.6 ± 0.1	0.6	10.5 ± 1	Non-stoichiometric TCP
C	1.5 ± 0.1	1.4	42.0 ± 5	Non-stoichiometric TCP

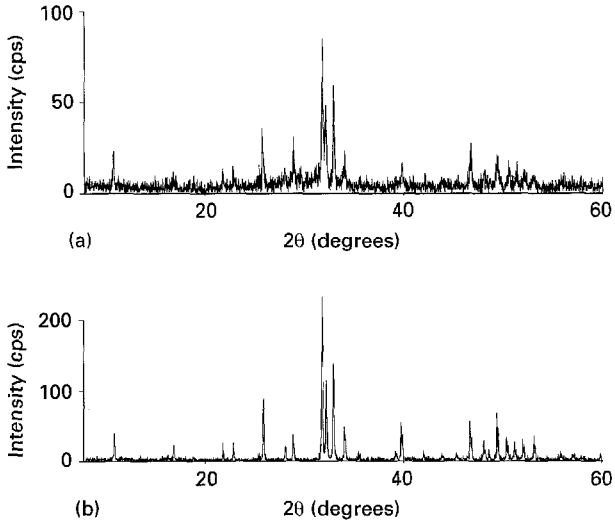

Figure 4 X-ray diffraction pattern (40 kV, 30 mA, scanning rate 0.02 degrees/s, CuK_α radiation) of (a) plasma-sprayed HA and (b) annealed plasma-sprayed HA (900 °C for 3 h).

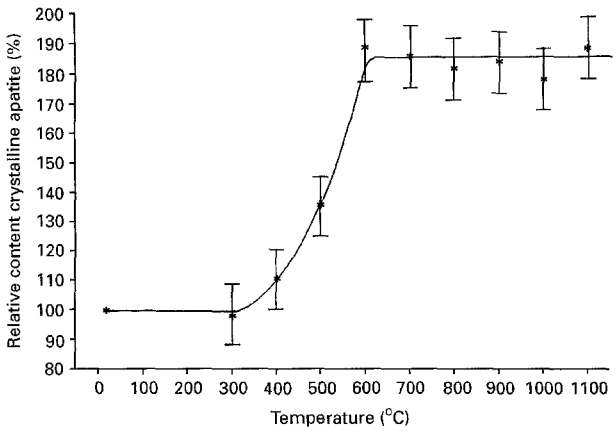

Figure 6 Relative content of crystalline apatite in the annealed plasma-sprayed samples as a function of temperature (obtained by the areas of the X-ray 3 0 0 reflexes of HA). 100% corresponds to the crystalline apatite content of the plasma-sprayed non-annealed sample.

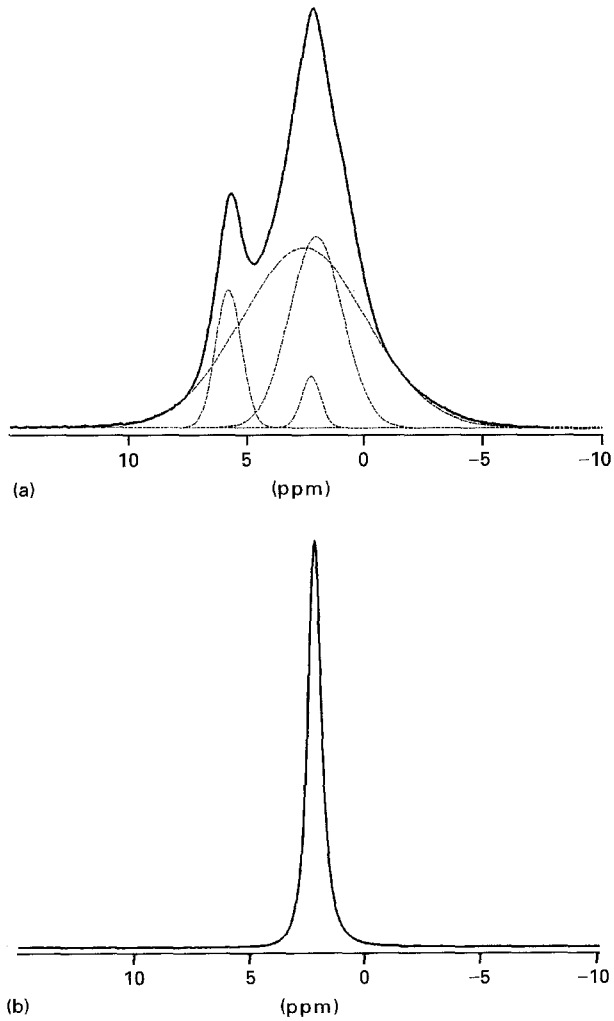

Figure 5 Experimental and simulated ^{31}P MAS-NMR spectra of (a) plasma-sprayed HA and (b) annealed (900 °C/3 h) plasma-sprayed HA (resonant frequency $\nu_0 = 161.92$ MHz; spinning speed $\nu_r = 14.0$ kHz; receiver delay time $t_{de} = 10$ μs; pulse width $t_w = 1.5$ μs and repetition time $t_{re} = 200$ s).

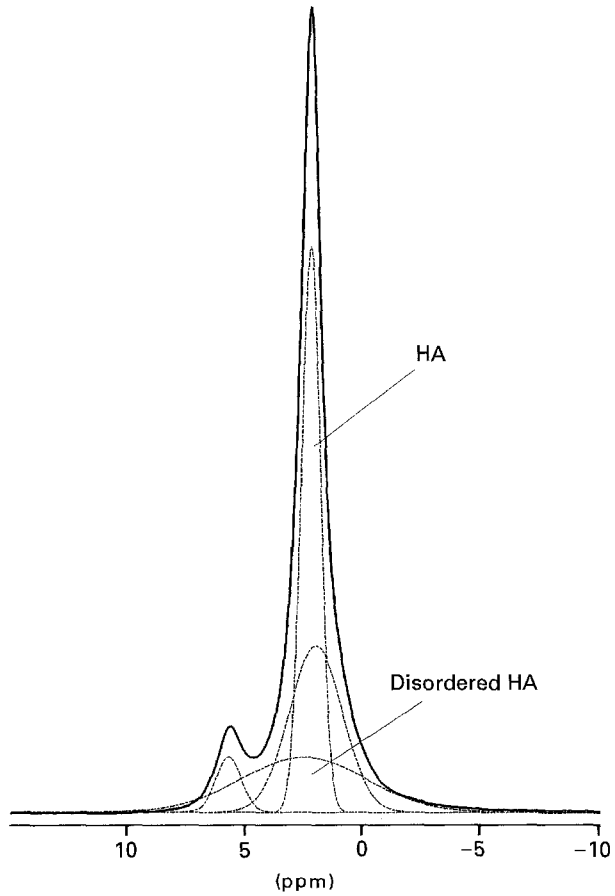

Figure 7 Experimental and simulated ^{31}P MAS-NMR spectrum of a plasma-sprayed annealed (400 °C/90 h) apatite (resonant frequency $\nu_0 = 161.92$ MHz; spinning speed $\nu_r = 14.0$ kHz; receiver delay time $t_{de} = 10$ μs; pulse width $t_w = 1.5$ μs and repetition time $t_{re} = 200$ s).

of an annealed sprayed sample (900 °C for 3 h) shows a single position at $\delta_{iso} = 2.4$ ppm and a MAS line width typical of crystalline apatite. The formation of TeCP or other phosphate phases during annealing of plasma-sprayed HA, described in [10], was not observed.

This reverse reaction depends on the temperature and time of the thermal treatment. In Fig. 6, the relative contents of crystalline HA in the annealed samples are presented as a function of temperature. In the range around 500 °C the content of crystalline HA

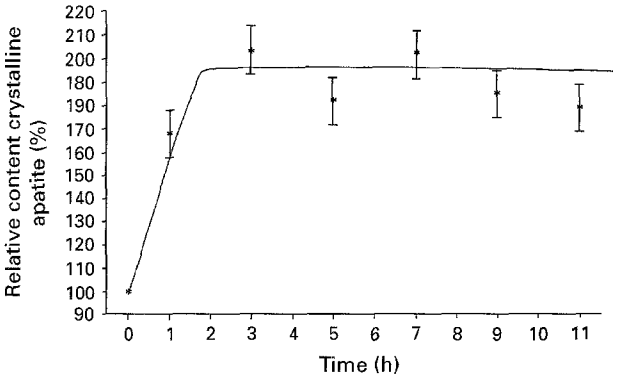

Figure 8 Relative content of crystalline apatite in the annealed plasma-sprayed samples as a function of time (obtained by the areas of the X-ray 3 0 0 reflexes of HA). 100% corresponds to the crystalline apatite content of the plasma-sprayed non-annealed sample.

increases strongly, and remains constant within the error limits after annealing at temperatures above 600 °C. To complete the reverse reaction at temperatures around 400 °C, a long annealing time is necessary. Fig. 7 shows the ^{31}P NMR-MAS spectrum of a sample annealed at 400 °C for 90 h. Comparison with the unannealed powder shows that the fitted line positions are retained during annealing, however, the relative intensities of the components clearly differ. As can be seen, the major part of both the distorted HA and the phase possessing a TCP-similar structure have been translated to crystalline HA during this temperature treatment. Fig. 8 gives the relative content of HA versus annealing time at a temperature of 800 °C. Within the first 2 h, the apatite content reaches a maximum. The value remains constant within error limits during further temperature treatment. The ^{31}P NMR measurements confirm the X-ray results.

Hexagonal titanium is transformed to the cubic modification at temperatures around 880 °C [12]. The annealing experiments described show that recrystallization of apatite in plasma-sprayed coatings clearly occurs below the phase transformation point of titanium. Therefore, correction of the crystallinity and phase composition of HA-coated titanium implants by thermal treatment should be possible without significant loss of strength.

First *in vitro* investigations indicate also an increase in chemical stability during annealing of plasma-sprayed hydroxyapatite.

4. Conclusions

Plasma spraying of apatite results in partial decomposition. Besides crystalline apatite, a considerable amount of distorted, partly X-ray amorphous apatite is formed. Additionally, an amorphous calcium phosphate phase, possessing a structure similar to TCP, can be observed. This phase should include an excess of calcium, because neither crystalline nor amorphous tetracalciumphosphate could be detected.

The decomposition of apatite during plasma spraying is reversible and can be described by a temperature and time dependent equilibrium reaction. Annealing of the plasma-sprayed material at temperatures around 500 °C or above results in a complete rebuild of the crystalline apatite structure.

References

1. J. F. OSBORN, E. KOVACS and A. KALLENBERGER, *Dtsch. Zahnärztl. Z.* **35** (1980) 54.
2. M. JARCHO, in Proceedings of the 1st International Bioceramic Symposium, Kyoto, April 1988 (Bioceramics, Vol. 1), edited by H. Oonishi, H. Aoki and K. Sawai (Ishiyaku Euro-America, Inc., Tokyo, St. Louis, 1989) pp. 57–61.
3. W. LACEFIELD, S. METSGER, N. BLUMENTHAL, P. DYCHEYNE, J. DAVIS, J. KAY, J. STEVENSON and R. SALSBURY, *J. Appl. Biomater.* **1** (1990) 84.
4. PAUCHIU E. WANG and T. K. CHAKI, *J. Mater. Sci. Mater. Med.* **4** (1993) 150.
5. J. WENG, X.-G. LIU, X.-D. LI and X.-D. ZHANG, *Biomaterials* **16** (1995) (1) 39.
6. J. VOGEL, P. HARTMANN, J. ALKEMPER, G. GÜNTHER and H. FUESS, *Glastech. Ber. Glass Sci. Technol.* **67C** (1994) 608.
7. S. R. RADIN and P. DYCHEYNE, *J. Mater. Sci. Mater. Med.* **3** (1992) 33.
8. P. HARTMANN, J. VOGEL and B. SCHNABEL, *J. Non-Cryst. Solids* **176** (1994) 157.
9. *Idem., J. Magn. Reson., Series A* **111** (1994) 110.
10. F. BROSSA, A. CIGADA, R. CHIESA, L. PARACCHINI and C. CONSONNI, *J. Mater. Sci. Mater. Med.* **5** (1994) 855.
11. J. ORTH, A. WILKE, M. KRAFT and P. GRISS, in Proceedings of the 4th International Symposium on Ceramics in Medicine, London, September 1991 (Bioceramics, Vol. 4), edited by W. Bonfield, G. W. Hastings and K. E. Tanner (Butterworth-Heinemann, Oxford, 1991) pp. 351–357.
12. "Handbook of chemistry and physics", 74th Edn (CRC Press, Boca Raton, FL, 1993/1994) pp. 4–31.

Received 15 September
and accepted 17 November 1995